Dynamically controlled optical nonreciprocity of a double-ladder system with spontaneously generated coherence in moving atomic optical lattice*

Nuo Ba(巴诺)[1,†], Xiang-Yao Wu(吴向尧)[1], Dong-Fei Li(李东飞)[1], Dan Wang(王丹)[1], Jin-You Fei(费金有)[1], and Lei Wang(王磊)[2]

[1] *College of Physics, Jilin Normal University, Siping* 136000, *China*
[2] *College of Physics, Jilin University, Changchun* 130012, *China*

(Received 2 November 2016; revised manuscript received 20 December 2016; published online 30 March 2017)

A four-level double-ladder cold atoms system with spontaneously generated coherence trapped in a moving optical lattice is explored to achieve optical nonreciprocity. When spontaneously generated coherence (SGC) is present, the remarkable contrast optical nonreciprocity of light transmission and reflection can be generated at each induced photonic bandgap in the optical lattice with a velocity of a few m/s. However, when the SGC effect is absent, the optical nonreciprocity becomes weak or even vanishing due to the strong absorption. It is found that the optical nonreciprocity is related to the asymmetric Doppler effect in transmission and reflection, meanwhile the degree and position of optical nonreciprocity can be tuned by the SGC effect and the Rabi frequency of the trigger field.

Keywords: atomic coherence, optical nonreciprocity, atomic lattice, photonic band gap

PACS: 42.50.Gy, 42.50.Wk, 42.70.Qs **DOI:** 10.1088/1674-1056/26/5/054207

1. Introduction

The effective approach to control light transport in artificial optical materials has been paid a great deal of attention in the last few decades for designing various photonic devices.[1,2] As a prominent artificial material, photonic crystal (PC)[3] possesses a photonic band gaps (PBG) structure, which has a dielectric constant periodically arranging in space and exhibits a series of marvelous behaviors about light propagation and interaction. However, in a traditional PC, the position and width of the PBG cannot be changed when the periodic structure is formed. So, people have proposed the use of electromagnetically induced transparency (EIT)[4] to obtain tunable PBG in cold atoms driven by a standing-wave field.[5–8] It is important to note that the spatially periodic coherent effect can be generated in cold atoms confined in an optical lattice.[9–14] In a theoretical paper, Petrosyan showed that such a system could induce a new PBG under the condition of EIT.[9] Whereafter, Schilke *et al*. have experimentally observed the Bragg reflection induced by PBG and characterized its dependency on the experimental parameters.[10,11] Recently, optical nonreciprocity based on tunable PBG has been studied extensively.[15,16] In fact, optical nonreciprocity of light transmission and reflection is impossible to generated in a linear and passive system. So, people have proposed various projects to achieve optical nonreciprocity, such as designing nonsymmetric photonic crystals[17] and exploring media with parity-time symmetry,[18] and media with magneto-optical effects.[19] In particular, some researches have shown that large optical nonreciprocity of transmission can be obtained by setting the photonic crystal[15] and exploiting the asymmetric Doppler shift in moving distributed atoms.[16,20,21] Optical nonreciprocity has the potential application in information processing, e.g., all-optical diodes[22,23] and unidirectional light transport.[24]

So far, most studies on the optical nonreciprocity effect are based on the laser induced atomic coherence,[16,20,21] and it is necessary to have at least one coupling field to form the atom coherence. However, spontaneously generated coherence (SGC) can also create the atomic coherence, while SGC refers to the quantum interference between spontaneous decay channels from closely placed upper levels to a ground level.[25,26] The SGC has been exploited to obtain amplification without inversion,[27,28] narrowing and quenching of spontaneous emission,[29,30] refractive index enhancement without absorption,[31] as well as coherent population transfer.[32] Recently, in many researches, people have achieved dynamically induced more PBGs[33–35] and electromagnetically induced gratings[36,37] as well as optical precursors[38] under the assistance of SGC. In this paper, we study the effect of SGC on the optical nonreciprocity of transmission and reflection in a moving optical lattice filled into a four-level ladder cold atoms system. By numerical calculation, we find that the atomic system has a significant optical nonreciprocity effect in two cases of resonant or off-resonant

*Project supported by the National Natural Science Foundation of China (Grant Nos. 11347137, 11247201, and 11247005) and the Twelfth Five-year Program for Science and Technology of Education Department of Jilin Province, China (Grant No. 20150215).

†Corresponding author. E-mail: banuo2008@163.com

© 2017 Chinese Physical Society and IOP Publishing Ltd

trigger field when SGC is present. However, the optical nonreciprocity effect seriously weakens when SGC is nonexistent. In addition, the degree of the nonreciprocity is related to the frequency difference of two close upper states, and the position of the nonreciprocity can be dynamically modulated by controlling the trigger field frequency.

2. Atomic model and relevant equations

The four-level double-ladder atomic system is shown in Fig. 1(a), where the closely lying doublet levels $|2\rangle$ and $|3\rangle$ have a frequency difference 2δ. A weak probe field propagating in the $\widehat{z}$ axis couples the ground state $|1\rangle$ with two closely lying upper levels $|2\rangle$ and $|3\rangle$, and the Rabi frequencies are $\Omega_{\rm p1} = \boldsymbol{E}_{\rm p}\cdot\boldsymbol{d}_{12}/2\hbar$ and $\Omega_{\rm p2} = \boldsymbol{E}_{\rm p}\cdot\boldsymbol{d}_{13}/2\hbar$. The levels $|2\rangle$ and $|3\rangle$ are simultaneously coupled to the excited state $|4\rangle$ by a trigger field propagating in the $\widehat{x}$ axis and the corresponding Rabi frequencies are $\Omega_{\rm T1} = \boldsymbol{E}_{\rm T}\cdot\boldsymbol{d}_{24}/2\hbar$ and $\Omega_{\rm T2} = \boldsymbol{E}_{\rm T}\cdot\boldsymbol{d}_{34}/2\hbar$, where $E_{\rm p}$ ($E_{\rm T}$) represents the amplitude of the probe (trigger) field and $\boldsymbol{d}_{ij}$ denotes the electric dipole moment of the transition $|i\rangle \to |j\rangle$. For simplicity, we assume in the following that the angle α between $\boldsymbol{d}_{12}$ and $\boldsymbol{d}_{13}$ is equally partitioned by $\boldsymbol{E}_{\rm p}$ while $\boldsymbol{d}_{34}$ is antiparalled to $\boldsymbol{d}_{24}$, as shown in Fig. 1(b). Then we set $d_{13}/d_{12} = p$, $d_{43}/d_{42} = q$, $\Omega_{\rm p1} = \Omega_{\rm p2}/p = \Omega_{\rm p}$, and $\Omega_{\rm T1} = \Omega_{\rm T2}/q = \Omega_{\rm T}$.

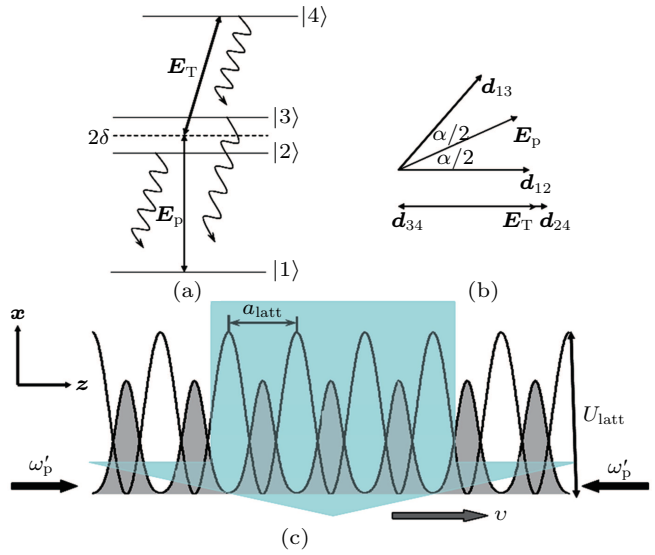


Fig. 1. (color online) (a) Schematic diagram of a four-level double Ladder-type system with two closely spaced upper levels $|2\rangle$ and $|3\rangle$ strongly coupled via spontaneous emission. (b) Arrangement of the probe (trigger) electric field $\boldsymbol{E}_{\rm p}$ ($\boldsymbol{E}_{\rm T}$) and the relevant dipole moments $\boldsymbol{d}_{12}$ and $\boldsymbol{d}_{13}$ ($\boldsymbol{d}_{24}$ and $\boldsymbol{d}_{34}$). (c) An atomic ensemble is filled into a 1D optical lattice of period $a_{\rm latt} = \lambda_{\rm latt}/2$ which is generated by a retroreflected laser beam with wavelength $\lambda_{\rm latt}$. The density of trapped atoms takes on a Gaussian distribution in each period of the 1D optical lattice. The probe and trigger fields propagate in the z axis and x axis, respectively. The 1D optical lattice is assumed to move with a velocity υ along its optical axis z.

Under the electric-dipole and rotating-wave approximations, according to the Weisskopf–Wigner theory of spontaneous emission, the probe susceptibility is derived by analytically solving the equations of motion for the probability amplitudes in a steady state, which can be written as

$$\chi(\omega_{\rm p}) = \left[\beta\frac{-\gamma_4'(p^2\gamma_2' + \gamma_3' - {\rm i}2p\gamma_{23}) + (p-q)^2\Omega_{\rm T}^2}{\gamma_4'(\gamma_2'\gamma_3' + \gamma_{23}^2) - \Omega_{\rm T}^2(q^2\gamma_2' + \gamma_3' - {\rm i}2q\gamma_{23})}\right], \quad (1)$$

where $\beta = ca_0\gamma_{21}/2\omega_{\rm p}$, $a_0 = N_0(z)|d_{24}|^2\omega_{\rm p}/(c\varepsilon_0\hbar\gamma_{21})$ is the absorption cross section, with $N_0(z)$ being the inhomogeneous atomic density as a function of position z, $\omega_{\rm p}$ is the probe frequency, $\gamma_{21} = \Gamma_2/2$, $\gamma_2' = \Delta_{\rm p} - \delta + {\rm i}\Gamma_2/2$, $\gamma_3' = \Delta_{\rm p} + \delta + {\rm i}\Gamma_3/2$, $\gamma_4' = \Delta_{\rm p} + \Delta_{\rm T} + {\rm i}\Gamma_4/2$, and $\gamma_{23} = k\sqrt{\Gamma_2\Gamma_3}/2$, with Γ_2, Γ_3, and Γ_4 being the spontaneous decay rates for the corresponding states. $\Delta_{\rm p} = \omega_{\rm p} - (\omega_{21} + \omega_{31})/2$ and $\Delta_{\rm T} = \omega_{\rm T} - (\omega_{42} + \omega_{43})/2$ denote the detunings of the probe and trigger fields, respectively. The cross coupling term between the two spontaneous emission pathways, which refers to SGC, is described as $k\sqrt{\Gamma_2\Gamma_3}/2$, where $k = \boldsymbol{d}_{12}\cdot\boldsymbol{d}_{13}/|\boldsymbol{d}_{12}||\boldsymbol{d}_{13}| = \cos\alpha$ is related to the alignment of the two spontaneous emission dipole matrix elements. When $\alpha = 0$ and $k = 1$, SGC is generated from the two decay channels, while if $\alpha = \pi/2$ and $k = 0$, there is no SGC.

Now we investigate the case that a great deal of cold atoms are trapped in the 1D optical lattice with period $a_{\rm latt}$ created by retroreflecting a laser beam of wavelength $\lambda_{\rm latt} = 2a_{\rm latt}$ along the z direction as shown in Fig. 1(c). The constant factor $\eta = U_0/k_{\rm B}T$ relies on the temperature of the atomic system T and the trapping depth of the optical potential U_0. In each period of the optical lattice, the atomic density exhibits a Gaussian distribution with width $\sigma(z) = \lambda_{\rm latt}/(2\pi\sqrt{\eta})$. It is noted that the wavelength of the optical lattice has $\lambda_{\rm latt} > \lambda_{31}$ to obtain the dipole traps. It reflects that the Bragg conditions $\lambda_0 = \lambda_{31}/\cos\theta$ can be satisfied and the little shift is defined as $\Delta\lambda_{\rm latt} = \lambda_{\rm latt} - \lambda_0$ for a propagation angle θ between the probe and the lattice beams which is nonzero. In the following, we use the transfer-matrix method to verify whether the induced PBGs depend on the SGC effect. First, we deduce the 2×2 unimodular transfer matrix m_j of the j-th single period, which can be divided into 100 sublayers with the same thickness δz for different densities $N(z_l)$ with ($l \in 1, 100$) and the transfer matrix of each sublayer can be written as

$$m_j(z_l) = \frac{1}{t_j(z_l)}\begin{bmatrix} t_j^2(z_l) - r_j^2(z_l) & r_j(z_l) \\ -r_j(z_l) & 1 \end{bmatrix}, \quad (2)$$

where $r_j(z_l)$ and $t_j(z_l)$ denote the elementary reflection and transmission coefficients, respectively. Then we obtain $M_j = m_j(z_1)\cdot m_j(z_2)\cdots m_j(z_{100})$. Second we can evaluate the transfer matrix M for the whole atomic medium of length $L = na_{\rm latt}$. It is simply to attain the probe reflectivities and transmissivities as

$$R_n(L) = \left|\frac{M_{(12)}}{M_{(22)}}\right|^2, \quad (3)$$

$$T_n(L) = \left|\frac{1}{M_{(22)}}\right|^2, \quad (4)$$

with $M_{(ij)}$ being one matrix element of the transfer matrix M.

It is noted that the density of states (DOS) for the probe photons can be reduced sufficiently when PBGs are opened up. The expression of DOS can be deduced using the method in Refs. [10] and [11], which can be written as

$$D(z) = \mathrm{Re}\left(\frac{2 + r_l(z) + r_r(z)}{1 - r_l(z) r_r(z)} - 1\right), \tag{5}$$

where $r_l(z)$ and $r_r(z)$ respectively denote the complex coefficients originated from photons ω_p emitting to the left and right ends of the 1D atomic lattices along the z direction.

Generally, the reflection and transmission of light are reciprocity in the rest frame. However, by considering the optical lattice moving with a constant velocity along its optical axis $\hat{z}$, with a given frequency ω' propagating along $\pm\hat{z}$ in the laboratory frame, the transmissivity $T(\omega')$ and refelectivity $R(\omega')$ are different in the two propagation directions due to the Doppler effect which leads to two different rest frame frequencies. For a Gaussian pulse with central frequency ω'_p and spatial length L' traveling along $+\hat{z}$ and $-\hat{z}$ through the moving optical lattice, the corresponding lab frame transmission and reflection can be expressed as

$$\begin{aligned} T_{\pm}(\omega'_p, L') &= \frac{L'}{c\sqrt{2\pi}} \int_{-\infty}^{\infty} \mathrm{d}\omega' \, \mathrm{e}^{-\left[(\omega'-\omega'_p)^2/2(c/L')^2\right]} \\ &\quad \times T\left((1 \mp \upsilon/c)\,\omega'\right), \end{aligned} \tag{6}$$

$$\begin{aligned} R_{\pm}(\omega'_p, L') &= \frac{L'}{c\sqrt{2\pi}} \int_{-\infty}^{\infty} \mathrm{d}\omega' \, \mathrm{e}^{-\left[(\omega'-\omega'_p)^2/2(c/L')^2\right]} \\ &\quad \times R\left((1 \mp \upsilon/c)\,\omega'\right). \end{aligned} \tag{7}$$

So the optical nonreciprocity in pulse transmission and reflection takes place as the forward and backward lights of frequency ω' are shift by $\mp\omega'(\upsilon/c)$, which can be defined as $\Delta T_p(\omega'_p, L') = T_+(\omega') - T_-(\omega')$, $\Delta R_p(\omega'_p, L') = R_+(\omega') - R_-(\omega')$. Then, we can expand $T(\omega)$ and $R(\omega)$ in Taylor series as

$$\begin{aligned} \Delta T(\omega'_p) &\approx -\upsilon/c \Big\{ 2\omega'_p \left[\mathrm{d}T(\omega'_p)/\mathrm{d}\omega\right] + (2c/L')^2 \\ &\quad \times \left[d^2 T(\omega'_p)/\mathrm{d}\omega^2\right] \Big\}, \end{aligned} \tag{8}$$

$$\begin{aligned} \Delta R(\omega'_p) &\approx -\upsilon/c \Big\{ 2\omega'_p \left[\mathrm{d}R(\omega'_p)/\mathrm{d}\omega\right] + (2c/L')^2 \\ &\quad \times \left[d^2 R(\omega'_p)/\mathrm{d}\omega^2\right] \Big\}, \end{aligned} \tag{9}$$

which mean that an appreciable degree of transmission and reflection nonreciprocity would require sharp frequency derivatives $|\mathrm{d}T(\omega)/\mathrm{d}\omega|$ and $|\mathrm{d}R(\omega)/\mathrm{d}\omega|$, respectively.

3. Numerical calculation and discussion

Now we investigate the effect of SGC on the probe susceptibility $\chi(\omega_p)$, and further show that the generation of PBGs and optical nonreciprocity are relevant to the SGC by numerical calculations. In Fig. 2, we plot the imaginary part of the susceptibility as a function of the probe detuning with and without SGC for resonant or off-resonant trigger field, respectively. According to Refs. [35] and [36], when the trigger field has a large detuning, i.e., $\Delta_T \gg \Gamma_4$ (which indicates a weak interaction between the trigger field and the system), the destructive quantum interference based on SGC leads to that all the population is trapped into dark state $|\Psi_{\mathrm{dark}}\rangle = \left[\delta|1\rangle + \Omega_p(|2\rangle - |3\rangle)\right]/\sqrt{\delta + 2\Omega_p^2}$. So a transparency window appears at $\Delta_p = 0$. Then, when the trigger field is resonant $\Delta_T = 0$, this means a strong interaction between the trigger field and the atom, which leads the single dark state $|\Psi_{\mathrm{dark}}\rangle$ to couple with level $|4\rangle$, so two dark states are obtained as $|\Psi_{\mathrm{dark}\pm}\rangle = \left[\delta|1\rangle + \Omega_p\left(|2\rangle - |3\rangle \mp \sqrt{2}|4\rangle\right)\right]/\sqrt{\delta + 2\Omega_p^2}$ at the frequencies of $\Delta_p = \pm\sqrt{2}\Omega_T$. Thus, we can see that two EIT windows are separated by a narrow absorption peak in Fig. 2(b). However, for the case of no SGC effect, the probe is partly absorbed in the single EIT window (see the black solid of the inset in Fig. 2(a)) and the two EIT windows (see the black solid of the inset in Fig. 2(b)).

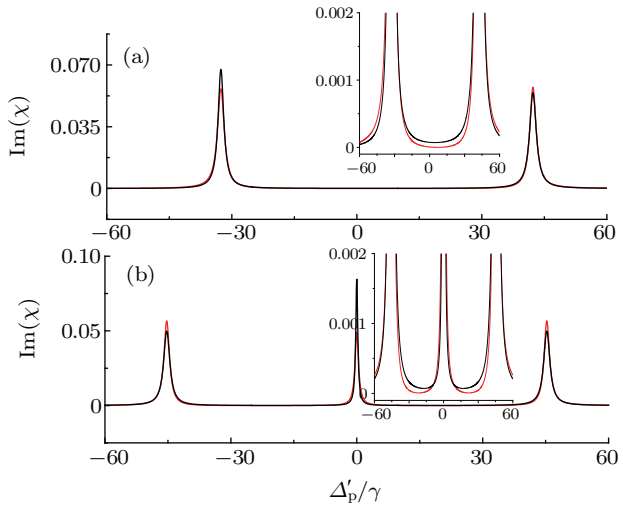


Fig. 2. (color online) The absorption spectra of probe field versus the normalized probe detuning Δ'_p/γ. The red and black lines correspond to the case with and without SGC, respectively. The relevant parameters are $\Gamma_2 = \Gamma_3 = \Gamma_4 = 2\gamma$, $\gamma = 1.0$ MHz, $\delta = 40.0\gamma$, $\Omega_T = 15\gamma$; (a) $\Delta_T = 60\gamma$, (b) $\Delta_T = 0$. The two insets display more detail about the probe absorption in the two cases.

As it is expected, owing to the Doppler effect and the forming PBGs, the probe transmission and reflection of the moving atomic lattice are changed. This will cause forward–backward nonreciprocity in probe transmission and reflection along the two propagation directions due to the Doppler frequency shifts. In the following, we explore how the SGC affects the pulse reflectivity and transmission and the optical nonreciprocity parameter for resonant and off-resonant trigger fields, respectively. In Fig. 3, we give the probe reflectivity and transmissivity spectra in its rest frame versus the probe detuning. We can see that when the trigger field is far away from resonant, one induced PBG is generated at $\Delta_p = 0$ due to the SGC effect (see the red line in Figs. 3(a) and 3(b)). However, when the trigger field is resonant, two symmetric PBGs

arise at $\Delta_p = \pm\sqrt{2}\Omega_T$, which are attributed to the trigger field and the SGC effect (see the red line in Figs. 3(c) and 3(d)). It is noted that when the SGC effect is absent, the pulse reflectivity and transmission are obviously decreased, therefore the PBGs are hardly formed (see the black line in Fig. 3). The physical mechanism for forming the PBG structure is that the SGC effect can induce a strongly transparent background for the off-resonant trigger field and the transparent background is divided into two EIT windows by the trigger for the resonant case. Figure 4 exhibits the nonreciprocity parameters of reflection $\Delta R\left(\omega_p'\right)$ and transmission $\Delta T\left(\omega_p'\right)$ for the probe field as a function of the probe detuning in the laboratory frame. We can see that in the presence of SGC, there is one large nonreciprocity parameter nearby $\Delta_p = 0$ for the off-resonant trigger field (see the red line in Figs. 4(a) and 4(b)), and two large nonreciprocity parameters arise in two frequency regions corresponding to $\Delta_p = \pm\sqrt{2}\Omega_T$ for the resonant case (see the red line in Figs. 4(c) and 4(d)). On the contrary, in the absence of SGC, the nonreciprocity effect clearly weakens and even disappears as shown by the black line in Fig. 4. Thus, the enhanced nonreciprocity parameters can be achieved in deeply narrow EIT windows which are induced by the SGC effect. In addition, we also discuss the nonreciprocity parameters as a function of the probe field detuning by changing the Rabi frequency of the trigger field Ω_T in Fig. 5. It is shown that the Rabi frequency of the trigger field has a significant role to play in controlling the positions of the nonreciprocity parameters. It is because the positions of the windows rely on the trigger field Rabi frequency, i.e., $\Delta_p = \pm\sqrt{2}\Omega_T$.

Figure 6 displays the densities of photonic states $D_+(z)$ and $D_-(z)$ as a function of the lattice position z with or without SGC for a resonant or off-resonant trigger field, where $+$ and $-$ denote a probe pulse traveling along the forward and backward of z, respectively. We can find that in the presence of SGC, $D_+(z)$ gradually decreases to nearly 0 in the integrating lattice length, while $D_-(z)$ becomes spatially periodically oscillating and related to the lattice position z. When SGC is absence, $D_+(z)$ is close to 0.4 for the off-resonant trigger field and approaches 0.1 for the resonant case, while the oscillation amplitude of $D_-(z)$ is gradually weak in the integrating lattice length. The reason is that when the forward probe field experiences a wide bandgap, the probe photons cannot penetrate the moving atomic lattice; while the backward probe field experiences a high transmission peak, the probe photons can propagate the atomic lattice with slow light. Figure 7 shows how the length of pulse L' and the moving velocity of atomic lattice υ affect the absolute value of the nonreciprocity parameter $|\Delta R|$ ($|\Delta T|$). We can find that when $L' > 200$ m and $\upsilon > 3$ m/s, $|\Delta R|$ and $|\Delta T|$ are both enhanced for the case with SGC. However, when SGC is absent, $|\Delta T|$ becomes very weak and $|\Delta R|$ has a large value in a small area. In addition, we show the relationship between the absolute value of the nonreciprocity parameter $|\Delta R|$ ($|\Delta T|$) with the frequency difference δ of the levels $|2\rangle$ and $|3\rangle$ in Fig. 8. We can see that the absolute value of the nonreciprocity parameter significantly increases and reaches above 90% in the vicinity of 40γ in the case of SGC (see the red line in Fig. 8). While the absolute value of the nonreciprocity parameter becomes small in the case of none SGC (see the black line in Fig. 8). Thus the frequency difference δ has an important effect on the degree of the nonreciprocity, because the widths of the transparent windows are related to the frequency difference δ.

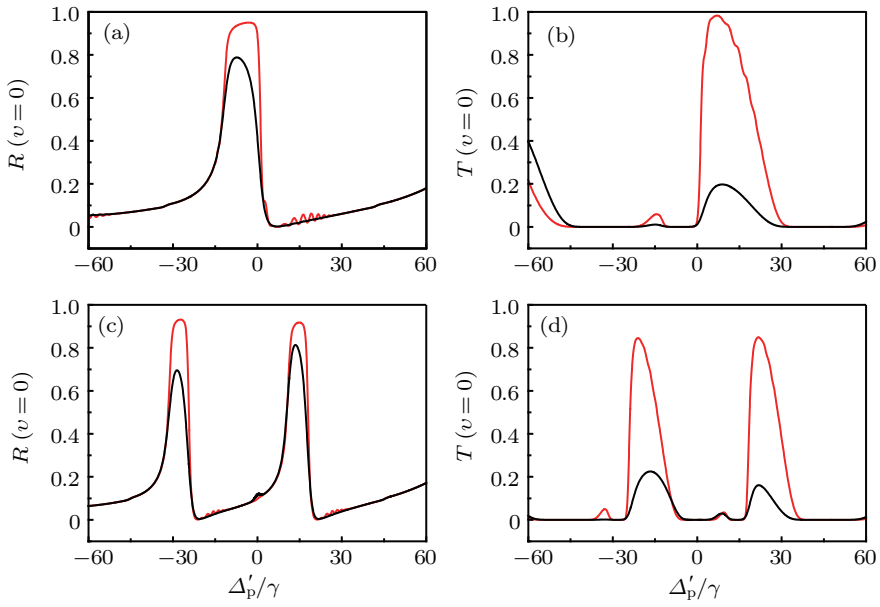


Fig. 3. (color online) The reflectivities and transmissivities of probe field in the rest frame for a 3.0 mm long sample, the atomic density is $N_0 = 1.0 \times 10^{12}$ cm^{-3} and $\lambda_{latt} = 780.787$ nm, $\Delta\lambda = 0.25$ nm, $\eta = 3.5$, (a), (b) for $\Delta_T = 60\gamma$; (c), (d) for $\Delta_T = 0$, the other parameters are the same as those in Fig. 2. The red and black lines correspond to the case with and without SGC, respectively.

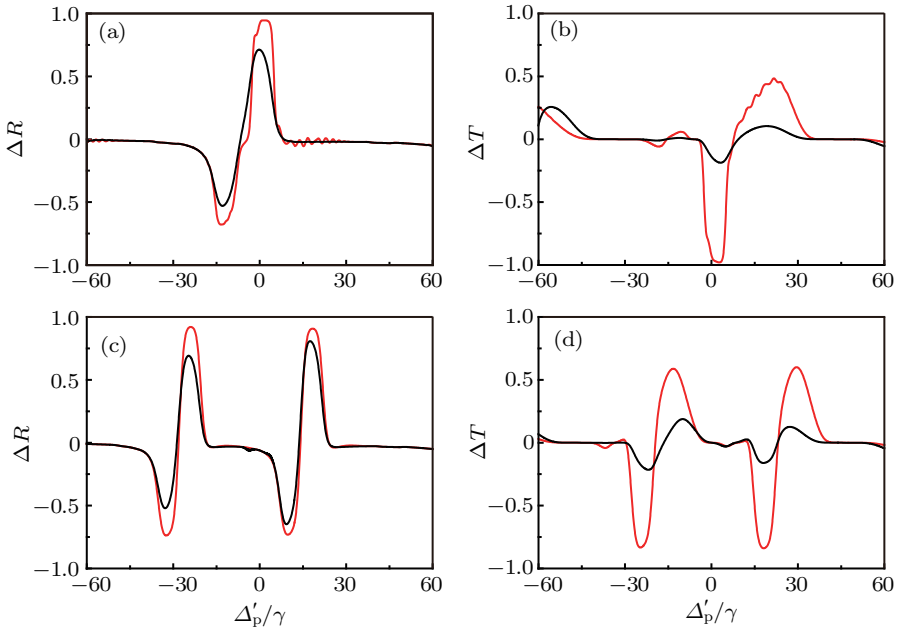


Fig. 4. (color online) The nonreciprocity parameters of reflection (ΔR) and transmission (ΔT) versus the normalized probe detuning for $\upsilon = 3$ m/s, with (a), (b) $\Delta_{\rm T} = 60\gamma$ and (c), (d) $\Delta_{\rm T} = 0$. The red and black lines correspond to the cases with and without SGC, respectively.

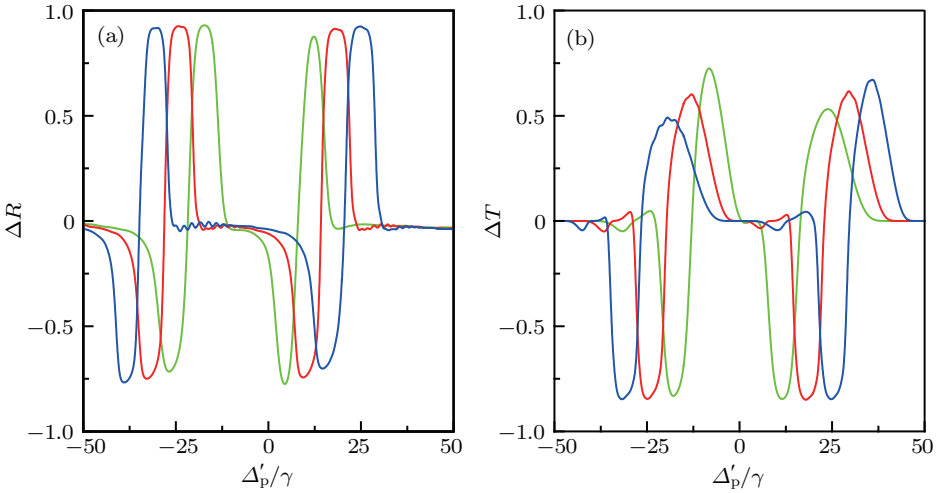


Fig. 5. (color online) The nonreciprocity parameters of (a) reflection (ΔR) and (b) transmission (ΔT) versus the normalized probe detuning for different Rabi frequencies of the trigger field with $\Omega_{\rm T} = 10\gamma$ (green solid), $\Omega_{\rm T} = 15\gamma$ (red solid), and $\Omega_{\rm T} = 20\gamma$ (blue solid), respectively, when the SGC is present and the trigger field is resonant.

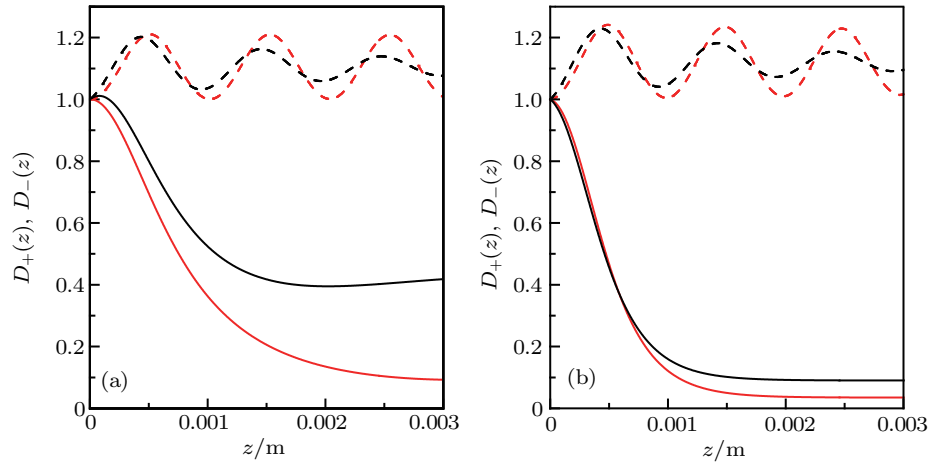


Fig. 6. (color online) Densities of states $D_+(z)$ (the solid line) and $D_-(z)$ (the dashed line) as a function of atomic lattice position z for $\Delta'_{\rm p} = 4.8\gamma$, $\Delta_{\rm T} = 60\gamma$ in panel (a); and $\Delta'_{\rm p} = 18.6\gamma$, $\Delta_{\rm T} = 0$ in panel (b). The red and black lines correspond to the cases with and without SGC, respectively.

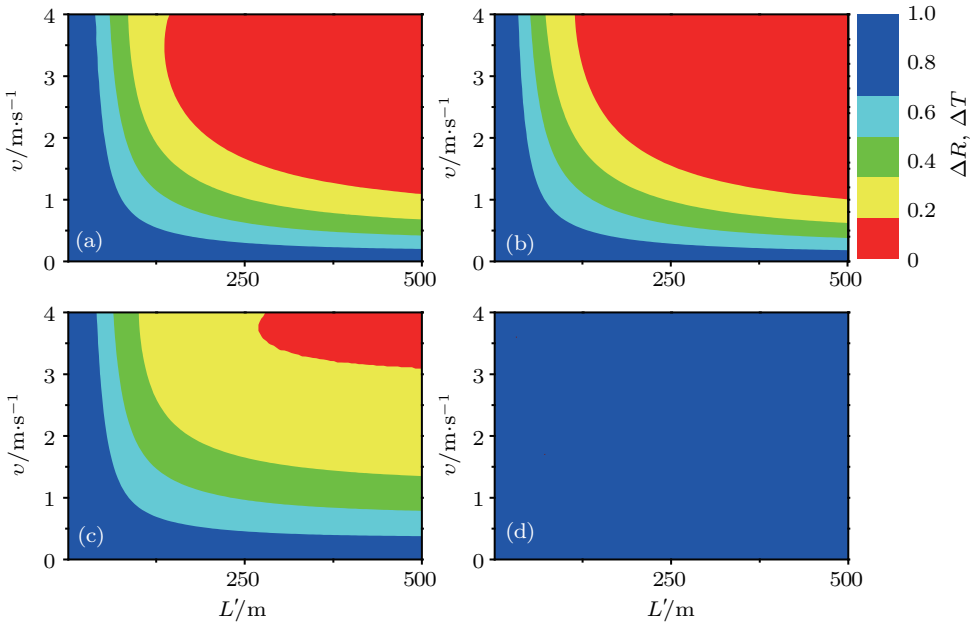


Fig. 7. (color online) The absolute values of nonreciprocity parameters of (a), (c) reflection ($|\Delta R|$) and (b), (d) transmission ($|\Delta T|$) versus the moving velocity of atomic lattice v and the pulse length L' for $\Delta'_{\rm p} = 18.6\gamma$ and $\Delta_{\rm T} = 0$. Panels (a) and (b) correspond to the case with SGC; and panels (c) and (d) correspond to the case without SGC.

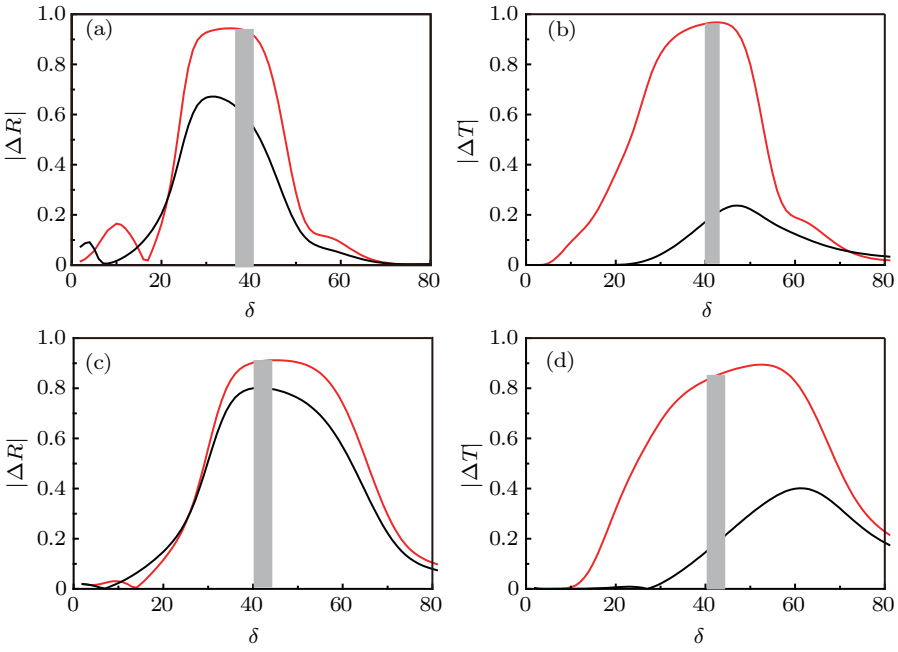


Fig. 8. (color online) The absolute values of optical nonreciprocity parameters $|\Delta R|$ and $|\Delta T|$ as functions of the frequency difference δ of the levels $|2\rangle$ and $|3\rangle$ for $\Delta'_{\rm p} = 4.8\gamma$, $\Delta_{\rm T} = 60\gamma$ in panels (a) and (b); and $\Delta'_{\rm p} = 18.6\gamma$, $\Delta_{\rm T} = 0$ in panels (c) and (d). The red and black lines correspond to the cases with and without SGC, respectively.

It is well known that it is hard to find a real atomic with near-degenerate levels and nonorthogonal dipole moments. However, the SGC could be obtained in charged quantum dots[39] and quantum wells[40] as well as the dressed-state picture of a coherently driven atom.[41–43] In fact, our discussed configuration with SGC is the same as the one given in Fig. 9(b) in the dressed-state picture of the coupling field $\Omega_{\rm c}$.[44] As a possible experiment, our studied system can be realized in the ^{87}Rb atom in Fig. 9(b), where the levels $|1\rangle$, $|2'\rangle$, $|3'\rangle$, and $|4\rangle$ correspond to $\left|5^2{\rm S}_{1/2}, F=1, m=-1\right\rangle$, $\left|5^2{\rm S}_{1/2}, F=2, m=+1\right\rangle$, $\left|5^2{\rm P}_{1/2}, F=1, m=0\right\rangle$, and $\left|5^2{\rm P}_{1/2}, F=2, m=+2\right\rangle$, respectively. It can be found that the two closely lying upper levels $|2\rangle$ and $|3\rangle$ in Fig. 9(a) may be seen as the coherent superposition of the levels $|2'\rangle$ and $|3'\rangle$ driven by $\Omega_{\rm c}$, i.e., $|2\rangle = \cos\theta\,|2'\rangle - \sin\theta\,|3'\rangle$ and $|3\rangle = \cos\theta\,|2'\rangle + \sin\theta\,|3'\rangle$, where $\tan\theta = \left(\Delta_{\rm c} + \sqrt{\Delta_{\rm c}^2 + 4\Omega_{\rm c}^2}\right)/2\Omega_{\rm c}$, with $\Delta_{\rm c}$ being the detuning of the field, and the frequency difference $2\delta = \sqrt{\Delta_{\rm c}^2 + 4\Omega_{\rm c}^2}$ can be manipulated.

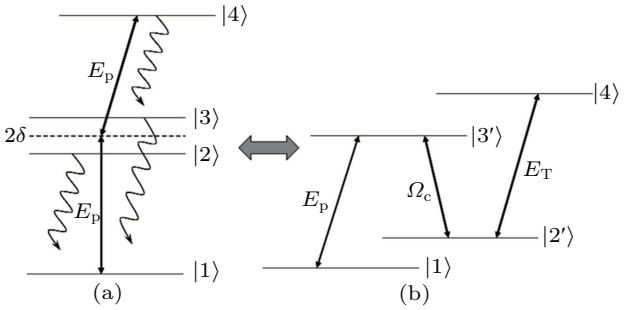


Fig. 9. (a) Four-level double ladder-type system with SGC. (b) A real four-level N-type atomic system. The former is equivalent to the latter in the dressed-state picture of the coupling field Ω_c.

4. Conclusion

We have investigated the optical nonreciprocity effect of a 1D moving atomic lattice with a Gaussian density distribution and exhibiting a four-level ladder type atomic system with SGC effect. It can be found that when the trigger field is far-resonant, one PBG with a large nonreciprocity effect can be formed in the transparency window by the SGC effect. When the trigger field is resonant, two well PBGs can lead to engendering two color nonreciprocal effects with SGC. However, when SGC is absent, the degree of nonreciprocal effect is declined obviously as the system absorbs strongly the probe field. We hope that these findings are helpful to design photonic devices, e.g., optical diodes, optical isolators, and invisible metamaterials.

References

[1] Oder T N, Shakya J, Lin J Y and Jiang H X 2003 *Appl. Phys. Lett.* **83** 1231
[2] Wu X, Yamilov A, Liu X, Li S, Dravid V P, Chang R P H and Cao H 2004 *Appl. Phys. Lett.* **85** 3657
[3] Istrate E and Sargent E H 2006 *Rev. Mod. Phys.* **78** 455
[4] Fleischhauer M, Imamoglu A and Marangos J P 2005 *Rev. Mod. Phys.* **77** 633
[5] Artoni M and La Rocca G C 2006 *Phys. Rev. Lett.* **96** 073905
[6] Wu J H, Artoni M and La Rocca G C 2008 *J. Opt. Soc. Am. B.* **25** 1840
[7] Zhang Y, Liu Y M, Tian X D, Zheng T Y and Wu J H 2015 *Phys. Rev. A* **91** 013826
[8] Zhang Y, Liu Y M, Han M, Wang G C, Cui C L and Zheng T Y 2014 *Acta Phys. Sin.* **63** 224203 (in Chinese)
[9] Petrosyan D 2007 *Phys. Rev. A* **76** 053823
[10] Schilke A, Zimmermann C, Courteille P W and Guerin W 2011 *Phys. Rev. Lett.* **106** 223903
[11] Schilke A, Zimmermann C and Guerin W 2012 *Phys. Rev. A* **86** 023809
[12] Yang H, Yang L, Wang X C, Cui C L, Zhang Y and Wu J H 2013 *Phys. Rev. A* **88** 063832
[13] Ba N, Wang L and Zhang Y 2014 *Acta Phys. Sin.* **63** 034209 (in Chinese)
[14] Wang D, Wu J Z and Zhang J X 2016 *Chin. Phys. B* **25** 064202
[15] Wang D W, Zhou H T, Guo M J, Zhang J X, Evers J and Zhu S Y 2013 *Phys. Rev. Lett.* **110** 093901
[16] Horsley S A R, Wu J H, Artoni M and La Rocca G C 2013 *Phys. Rev. Lett.* **110** 223602
[17] Serebryannikov A E 2009 *Phys. Rev. B* **80** 155117
[18] Feng L, Xu Y L, Fegadolli W S, Lu M H, Oliveira J E B, Almeida V R, Chen Y F and Scherer A 2013 *Nat. Mater.* **12** 108
[19] Zaman T P, Guo X and Ram R J 2007 *Appl. Phys. Lett.* **90** 023514
[20] Yang L, Zhang Y, Yan X B, Sheng Y, Cui C L and Wu J H 2015 *Phys. Rev. A* **92** 053859
[21] Sheng Y, Yang L, Yan X B, Wu J H and Cui C L 2015 *Opt. Commun.* **338** 479
[22] Zhou H, Zhou K F, Hu W, Guo Q, Lan S, Lin X S and Gopal A V 2006 *J. Appl. Phys.* **99** 123111
[23] Lin X S, Yan J H, Wu L J and Lan S 2008 *Opt. Express* **16** 20949
[24] Alberucci A and Assanto G 2008 *Opt. Lett.* **33** 1641
[25] Menon S and Argarwal G S 1998 *Phys. Rev. A* **57** 4014
[26] Paspalakis E and Knight P L L 1998 *Phys. Rev. Lett.* **81** 293
[27] Xu W H, Wu J H and Gao J Y 2002 *Phys. Rev. A* **66** 063812
[28] Wu J H and Gao J Y 2002 *Phys. Rev. A* **65** 063807
[29] Zhu S Y, Chan R C F and Lee C P 1995 *Phys. Rev. A* **52** 710
[30] Kapale K T, Scully M O, Zhu S Y and Zubairy M S 2003 *Phys. Rev. A* **67** 023804
[31] Xu W H, Wu J H and Gao J Y 2004 *Eur. Phys. J. D* **30** 137
[32] Yang X H and Zhu S Y 2008 *Phys. Rev. A* **77** 063822
[33] Gao J W, Zhang Y, Ba N, Cui C L and Wu J H 2010 *Opt. Lett.* **35** 709
[34] Gao J W, Bao Q Q, Wan R G, Cui C L and Wu J H 2011 *Phys. Rev. A* **83** 053815
[35] Yao Y P, Zhang T Y, Kou J and Wan R G 2013 *Phys. Lett. A* **377** 1416
[36] Wan R G, Kou J, Jiang L, Jiang Y and Gao J Y 2011 *Phys. Rev. A* **83** 033824
[37] Ba N, Wang L, Wu X Y, Liu X J, Wang H H, Cui C L and Li A J 2013 *Appl. Opt.* **52** 4264
[38] Ba N, Wang L, Wang H H, Li D F, Wang D and Yan L Y 2016 *Acta Phys. Sin.* **65** 014201 (in Chinese)
[39] Dutt M V, Cheng J, Li B, Xu X, Li X, Berman P R, Steel D G, Bracker A S, Gammon D, Economou S E, Liu R B and Sham L J 2005 *Phys. Rev. Lett.* **94** 227403
[40] Wu J H, Gao J Y, Xu J H, Silvestri L, Artoni M, LaRocca G C and Bassani F 2005 *Phys. Rev. Lett.* **95** 057401
[41] Ficek Z and Swain S 2004 *Phys. Rev. A* **69** 023401
[42] Wu J H, Li A J, Ding Y, Zhao Y C and Gao J Y 2005 *Phys. Rev. A* **72** 023802
[43] Zhang Y, Liu Y M, Zheng T Y and Wu J H 2016 *Phys. Rev. A* **94** 013836
[44] Schmidt H and Imamoglu A 1996 *Opt. Lett.* **21** 1936